

Planar KrF Laser-Induced OH Fluorescence Imaging in a Supersonic Combustion Tunnel

T. M. Quagliaroli,* G. Laufer,† S. D. Hollo,‡ R. H. Krauss,§ R. B. Whitehurst III,‡ and J. C. McDaniel Jr.†
University of Virginia, Charlottesville, Virginia 22903

Planar fluorescence images of OH were obtained in a continuous-flow, electrically heated, high enthalpy, hydrogen-air combustion tunnel, using a tunable KrF laser. These images were compared to previously recorded fluorescence images produced using a doubled-dye laser under similar conditions. For the detection configuration used, the images of doubled-dye laser-induced fluorescence demonstrated a severe distortion as a result of laser beam absorption and fluorescence trapping. By contrast, images of the fluorescence induced by the tunable KrF laser retained the symmetry properties of the flow. Based on signal-to-noise ratio measurements, the yield of the fluorescence obtained with the doubled-dye laser is considerably larger than the fluorescence yield induced by the KrF laser. The measurement uncertainties in the present facility of OH fluorescence induced by the KrF laser were primarily controlled by photon-statistical noise. Based on these results, tunable KrF laser systems are recommended for quantitative OH imaging in facilities where the product of the optical path length for either fluorescence excitation or collection and the average OH concentration along that path is greater than 10^{16} cm/cm³.

Introduction

THE development of the supersonic combustion ramjet (scramjet) requires measurements of the mixing and combustion of hydrogen in high stagnation temperature supersonic flow facilities. Laser-induced fluorescence (LIF) techniques are widely used for quantitative, nonintrusive, spatially resolved, instantaneous, or time-averaged measurement of flow temperature and density variations of the probed molecules. LIF techniques usually provide the high-signal-to-noise ratio (SNR) necessary for planar imaging in mixing and reacting regions. Several molecules that are present in hydrogen-air combustion are resonant with existing lasers and are therefore accessible for LIF measurements. Most notable are O₂,^{1,2} OH,³ and NO.^{4,5} Since the hydroxyl radical OH is formed only after the onset of the reaction, it can serve as an excellent marker of the reaction zone and its thermodynamic properties, and as an indicator of the progress of the combustion process. LIF measurements of OH present potential for imaging of temperature, density, and velocity fields in supersonic combustion facilities. However, characteristics of high-speed flows in combustion tunnels or engines, where abrupt variations in pressure and density often occur, may introduce significant systematic errors in density and temperature measurements. These errors are caused by one or more of the following; large variations in fluorescence due to collisional quenching, Doppler shift of the absorption frequency, and attenuation by media which may be optically thick for incident and/or emitted radiation. Although the effect of some of these errors may be reduced when symmetry or convenient optical

access is available, they still may not be correctable in many nonlaboratory scale experiments without full knowledge of the distribution of flow composition, velocity, pressure, and temperature. The systematic errors induced by these effects are additive to the noise-induced uncertainty and may severely restrict the application range and the accuracy of quantitative LIF measurements involving OH.

Several types of facilities are currently available for scramjet testing.⁶ Two of these types of facilities, the vitiated air and the electrically heated air facilities, can permit continuous testing at moderate Mach numbers and total temperatures to approximately 2000 K. Pulsed shock tunnel facilities allow total temperatures on the order of 5000 K and testing to Mach 20 and above.⁷ Two laser systems are available for OH LIF measurements in these facilities. A Nd:YAG-pumped, frequency-doubled dye laser system can be used for the excitation of most OH transitions in the $A^2\Sigma^+ \leftarrow X^2\Pi$ band. However, owing to its moderate pulse energy (≈ 40 mJ) it has been most often used to excite transitions near 290 nm. These transitions offer high fluorescence yield, accompanied by a high probability for collisional quenching.³ Alternatively, a tunable KrF laser system, operating near 248 nm, can be used to excite strongly predissociated transitions of OH where the uncertainty associated with collisional quenching is minimized, at the expense of a reduction in the fluorescence signal intensity.⁸

The performance of these two OH LIF techniques in supersonic combustion facilities has been evaluated theoretically and application criteria have been identified.⁹ Attenuation by absorption of the incident laser beam and trapping of the fluorescence by OH molecules along the detection path were predicted to seriously influence LIF measurements in some experimental situations. Coincidentally, these effects appeared to be more significant for transitions which are also susceptible to quenching. For example, the combined effects of attenuation of an incident doubled-dye laser beam, tuned to a rovibronic transition in the $A^2\Sigma^+(v' = 1) \leftarrow X^2\Pi(v'' = 0)$ band and trapping of the fluorescence detected in the $1 \rightarrow 1$ and $0 \rightarrow 0$ bands exceeds 70% when the incident beam and the emitted fluorescence travel through 10 cm OH at a concentration of 2×10^{15} cm⁻³ and a temperature⁹ of 2000 K. The loss caused by the attenuation effects is additive to the losses due to collisional quenching. Conversely, for excitation by the KrF laser in the $3 \leftarrow 0$ and detection in the $3 \rightarrow 3$ or

Presented as Paper 92-3346 at the AIAA/SAE/ASME/ASE 28th Joint Propulsion Conference and Exhibit, Nashville, TN, July 6–8, 1992; received July 13, 1992; revision received Nov. 19, 1993; accepted for publication Nov. 30, 1993. Copyright © 1992 by the authors. Published by the American Institute of Aeronautics and Astronautics, Inc., with permission.

*Research Assistant, Aerospace Research Laboratory, 570 Edgemont Rd. Student Member AIAA.

†Associate Professor, Aerospace Research Laboratory, 570 Edgemont Rd. Member AIAA.

‡Research Scientist, Aerospace Research Laboratory, 570 Edgemont Rd. Member AIAA.

§Research Associate Professor, Aerospace Research Laboratory, 570 Edgemont Rd. Member AIAA.

the $3 \rightarrow 2$ bands, the total attenuation by absorption and trapping is less than 1% for a similar configuration.⁹ Thus, it is predicted that a significant distortion of the OH fluorescence images induced by the doubled-dye laser system may be encountered in tests in many supersonic combustion facilities. The selection of a suitable LIF technique is strongly coupled to the flow conditions and the physical restrictions (e.g., optical access) imposed on the experimental configuration by the test facility itself. In addition to the generally recognized effects of collisional quenching, errors associated with absorption and trapping must be considered to avoid serious distortion of the measured results.

Two OH vibrational bands were selected to demonstrate the effects of attenuation and trapping on PLIF measurements. The first is the excitation of the $A^2\Sigma^+(v' = 1) \leftarrow X^2\Pi(v'' = 0)$ band, followed by detection in the $1 \rightarrow 1$ and $0 \rightarrow 0$ bands. This transition has been used most often for excitation by doubled-dye lasers. It has been identified⁹ as being subject to extensive attenuation and trapping losses even when the OH density and the optical path length are moderate. The other transition demonstrated here is in the $A^2\Sigma^+(v' = 3) \leftarrow X^2\Pi(v'' = 0)$ band, followed by detection of the $3 \rightarrow 2$ or $3 \rightarrow 3$ band. Although this technique produces significantly less signal, the effects of quenching and attenuation by laser absorption and fluorescence trapping are minimal, even in media that appear optically thick to the $1 \leftarrow 0$ transition. The PLIF images obtained by these two techniques were compared in a 3×3.8 cm, continuous-flow, electrically heated, high enthalpy hydrogen-air combustion tunnel. The results presented here are also the first demonstration of OH fluorescence imaging induced by a tunable KrF laser system in a supersonic combustion facility.

Theoretical Background

The fluorescence process generally used for OH PLIF involves the excitation of the $X^2\Pi(v'' = 0)$ state of OH to the $A^2\Sigma^+$ electronic state. Depending on the excitation wavelength, the $v' = 0, 1, 2,$ or 3 vibrational levels in the $A^2\Sigma^+$ state can be excited. For these four bands, the Einstein B coefficient is the largest for the $A^2\Sigma^+(v' = 0) \leftarrow X^2\Pi(v'' = 0)$ absorption, and the smallest for the $A^2\Sigma^+(v' = 3) \leftarrow X^2\Pi(v'' = 0)$ absorption. Therefore, most excitations of the $v' = 0$ level are expected to yield larger excited state population and potentially larger fluorescence signal than the excitation of the $v' = 3$ level. Doubled-dye laser systems can be designed to excite any of the OH transitions in the $A^2\Sigma^+(v' = 0, 1, 2,$ or $3) \leftarrow X^2\Pi(v'' = 0, 1)$ vibronic bands. However, owing to the relatively low pulse energy of these lasers, excitation of the strongly absorbing $A^2\Sigma^+(v' = 1) \leftarrow X^2\Pi(v'' = 0)$ transition was most often used for LIF¹⁰⁻¹³ and PLIF^{3,14-16}. The $0 \leftarrow 0$ excitation is highly absorbing and is not recommended¹⁷ for measurements in most combustion facilities. On the other hand, the tunable KrF laser is resonant only with rotational transitions in the $A^2\Sigma^+(v' = 3) \leftarrow X^2\Pi(v'' = 0)$ band. The higher pulse energy of this laser partially compensates for the relatively weak absorption of this band.

Following excitation, molecules may radiate by decaying to any of the vibrational levels in the ground electronic state. For the excitation of the $1 \leftarrow 0$ band, transitions in the $1 \rightarrow 1$ or $0 \rightarrow 0$ vibronic bands are normally detected.³ Other radiative transitions from $v' = 1$ to $v'' \neq 1$ are detectable,¹⁸ but should be avoided for reasons to be explained below. For excitation induced by the tunable KrF laser, the $3 \rightarrow 2$ or $3 \rightarrow 3$ bands are normally detected.⁸ The final state of the fluorescence transition following the excitation by the KrF laser is higher in energy than the final state following excitation of the $0 \leftarrow 0$ or $1 \leftarrow 0$ bands by the doubled-dye laser. Thus, the fluorescence induced by the KrF laser is less likely to be reabsorbed (trapped) by the lower population of OH molecules in these states along the detection path, even when the concentration and temperature of OH are high.

Excitation of the $A^2\Sigma^+(v' = 2) \leftarrow X^2\Pi(v'' = 0)$ band was also considered an alternative to the $1 \leftarrow 0$ and $3 \leftarrow 0$ excitation methods. The $2 \leftarrow 0$ absorption is weaker than the $1 \leftarrow 0$ absorption, thereby reducing the effect of laser beam attenuation. In addition, to reduce the effects of fluorescence trapping, narrow band spectral filtering should be used to resolve fluorescence in the $2 \rightarrow 2$ or $2 \rightarrow 1$ bands from the strongly trapped $0 \rightarrow 0, 1 \rightarrow 1,$ and possibly $1 \rightarrow 0$ bands following decay from the $v' = 2$ level to the $v' = 1$ and $v' = 0$ levels by vibrational energy transfer (VET). Calculations⁹ suggest that trapping may be significantly reduced if fluorescence from $v' = 2$ is isolated from fluorescence from $v' = 1$ and $v' = 0$. However, if the isolation is successful, other problems still remain. Molecules removed from $v' = 2$ by VET will not contribute to the detected fluorescence. Thus, the VET of the $v' = 2$ level is combined with the collisional removal of excited molecules from the electronic state. The rates for VET¹⁹ can be significantly different and are independent from collisional quenching effects of the electronic state.²⁰ For example, the cross section for VET¹⁹ from $v' = 1$ for collision with N_2 at 300 K is 26 \AA^2 , whereas the cross section for electronic quenching²⁰ by N_2 is only 2.5 \AA^2 . Conversely, the cross section for electronic quenching by H_2O is 76 \AA^2 , whereas for VET by H_2O ¹⁹ it is $<14 \text{ \AA}^2$. Since the lifetime in the $v' = 2$ state is 50 ns or longer,²¹ measurement of the fluorescence from $v' = 2$ in atmospheric pressure flames will depend strongly on the local composition and temperature. Also, correction for quenching will have to include VET by N_2 and electronic quenching by H_2O . Similarly, if transitions in the $v' = 1 \rightarrow v'' \neq 1$ band are detected following the excitation of $v' = 1$, effects of both VET and electronic quenching must be considered. On the other hand, for simultaneous detection of the $1 \rightarrow 1$ and $0 \rightarrow 0$ transitions, only electronic quenching may need to be considered and may be largely corrected for by assuming, for high H_2O concentrations, that the total quenching rate in the flow can be approximated collisions with H_2O alone.²⁰ This added complexity associated with VET is expected to seriously inhibit quantitative OH density and temperature measurements using excitation of $v' = 1$ or 2 followed by $v' \rightarrow v'' \neq v'$ detection in atmospheric flames.

The equations used to determine the amount of fluorescence signal detected by an electronic camera, the extent of the laser energy absorbed by OH along the beam path, and the amount of fluorescence trapping along the detection path have been described in detail.⁹ The number of fluorescence photons N_p that would be collected by a camera lens, following trapping losses, and focused on a detection array were determined for a range of experimental conditions.⁹

In most OH LIF experiments, the statistical nature of the photodetection is expected to be the primary noise source. Other noise sources will either increase with the photon statistical noise²² or be relatively small when the signal level is low. The number of photoelectrons imaged at each pixel of the detection array would then be the product of N_p and the photocathode quantum efficiency η_{pc} . The SNR is then

$$\text{SNR} = \sqrt{2} \eta_{pc} N_p \quad (1)$$

where the factor of $\sqrt{2}$ was included to account for the increase in the noise that is introduced by the high gain amplification of the intensifier of electronic cameras.²² When the intensifier gain is low, or for detection by photomultiplier tubes (PMT), this factor is omitted. In most experiments, external noise sources can be well controlled. Therefore, when the signal is low, the SNR is dominated by the photon-statistical noise and is proportional to the square-root of the signal. As the signal increases, the relative contribution of the photon-statistical noise decreases, and other noise parameters such as digitization noise or electromagnetic noise become dominant. In most fluorescence applications, where low signals are typical, the photon-statistical noise is the controlling

parameter of the overall noise. Thus, measurements of the SNR represent an indirect measurement of the signal itself and can be used to estimate the signal collected by a PMT or at each pixel of an intensified camera without the need for photometric measurements.²³

Results

The effects of attenuation and trapping on planar LIF images induced by the doubled-dye and tunable KrF laser systems were demonstrated in a 3×3.8 -cm, continuous-flow, electrically heated, high-enthalpy, hydrogen-air combustion tunnel. Two transitions, the $1 \leftarrow 0$ and the $3 \leftarrow 0$, were selected for this demonstration. The first transition was excited by a doubled-dye laser system, followed by detection in the $1 \rightarrow 1$ and $0 \rightarrow 0$ bands, to minimize effects of quenching.²⁴ The $3 \leftarrow 0$ band was excited by a tunable KrF laser. Figure 1 presents the illumination and detection configuration. The laser beam has been introduced through a side window (labeled observation window in the figure), and emerged through the exit window at the opposite side. For conventional excitation of the $1 \leftarrow 0$ band, beam attenuation of up to 30% is predicted, depending on the OH concentration and the gas temperature. The results of previously reported experiments²⁴ were used for comparison with the results of the present work. To reproduce the previously reported experimental setup, the camera was placed at the observation window at an angle of 45 deg to the incident light sheet. Although trapping of up to 43% is expected⁹ for detection normal to the beam, it may not even be evident if it is symmetric across the image. However, with this configuration, fluorescence emitted next to the exit window was detected through a larger depth of OH-rich gas than the fluorescence emitted next to the observation window. Therefore, the loss of signal seen in the region near the exit window exceeds the attenuation of the signal in the region next to the observation window. This effect is combined with attenuation by absorption of the incident laser beam. Although this detection arrangement is less often used in PLIF experiments, it has the advantage of visually demonstrating the potential effect of fluorescence trapping in large facilities.

Figure 2 presents two PLIF OH images averaged over eight laser pulses. The image obtained by tuning the doubled-dye laser to the $Q_1(6) 1 \leftarrow 0$ transition is from a previously reported experiment.²⁴ The second image was obtained by tuning the KrF laser to the $P_1(8) 3 \leftarrow 0$ line after reproducing

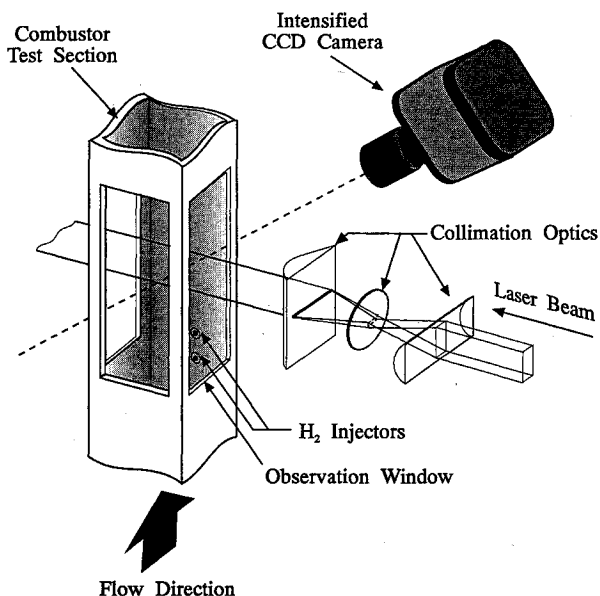


Fig. 1 Schematic of the experimental configuration for the imaging of OH in a supersonic combustion tunnel. The main flow is from below. Hydrogen is injected through two ports in the block wall.

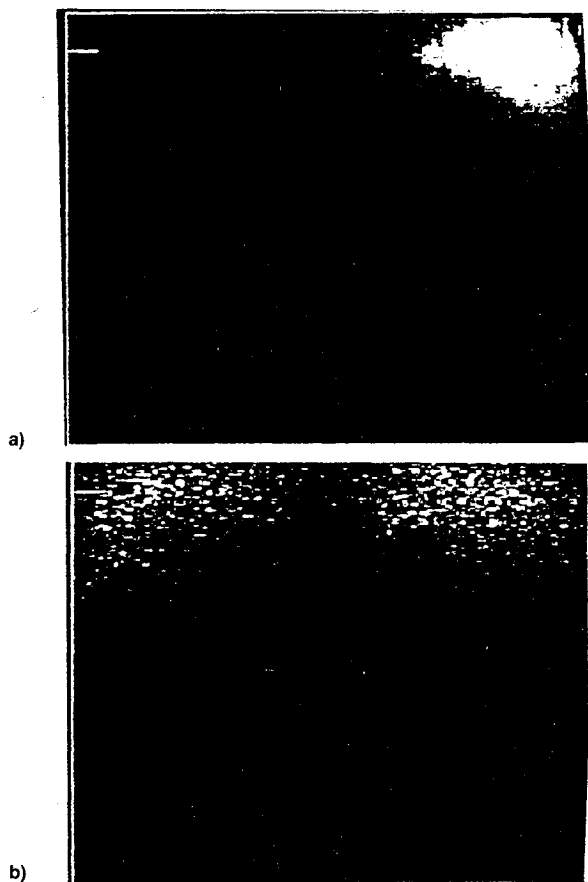


Fig. 2 OH PLIF images obtained in a supersonic combustive flow by a) (dye laser) the excitation of the $Q_1(6) 1 \leftarrow 0$ band with detection of the $1 \rightarrow 1$ emission band, and by b) (KrF laser) the excitation of the $3 \leftarrow 0$ band with detection of the $3 \rightarrow 2$ emission band.

the flow and imaging conditions of Ref. 24. This is the first demonstration of OH fluorescence imaging of a supersonic combustive flow induced by a KrF laser. Both images are of the crossflow OH distribution in a Mach 2, H_2 -air flame, downstream of a rearward-facing step. Fuel injection is through circular, staged, sonic injectors located at 3 and 7 step heights downstream of the rearward-facing step. The image plane is 4 step heights downstream of the first injector, at the centerline of the second injector. The main flow of preheated air in these images is directed normal to the page and the H_2 fuel is injected from the top. The freestream Mach number for both experiments was $M_\infty = 2$, the stagnation pressure and temperature were 390 KPa and 670 K, respectively, and the fuel flow rate was 0.55 gm/s. The injection dynamic-pressure ratio was 1.87 when the KrF laser was used and 1.5 in the experiment where the doubled-dye laser was used.²⁴ The incident energy of the KrF laser was 59 mJ/pulse, formed into a light sheet 2 cm wide and 0.1 mm thick. The incident energy of the doubled-dye laser was 0.7 mJ/pulse, formed into a light-sheet 2.5 cm wide and 0.1 mm thick. The fluorescence signal was separated from elastically scattered light and flame luminosity by bandpass filters with a peak transmission of $\sim 20\%$. In both experiments the images were captured through a uv, 105-mm, f/4.5, camera lens with an aperture of 2.54 cm placed at a distance of 35 cm from the center of the illumination light sheet. The images were corrected for the spatial distortion introduced by the oblique detection and for background radiation. In the images induced by the KrF laser each pixel represents a 0.23×0.23 -mm section in the flow. In the images induced by the doubled-dye laser each pixel represents a 0.20×0.20 -mm section in the flow.

It is evident from Fig. 2 that the image of the fluorescence induced by the KrF laser is symmetric with respect to the

symmetry plane defined by the injection jets. In contrast, the combination of attenuation and trapping has strongly distorted the fluorescence image produced by the doubled-dye laser, where only one flame lobe is visible. Clearly, the images obtained with the dye laser system do not provide even a qualitative picture of this flame. A perpendicular detection scheme would approximately equalize the detection path lengths from all points on the laser sheet. The fluorescence trapping would then become approximately symmetric, reducing or even eliminating visible loss effects. However, even if not visible, errors due to trapping may exceed 40% and will depend on the distance of the imaged plane from the detection system.

This comparison confirms a theoretical prediction⁹ that absorption by OH of the KrF laser beam and the trapping of the fluorescence induced by it are significantly less than that of the doubled-dye laser. For further comparison, Fig. 3 shows the variation of the relative fluorescence intensity across the test section along a line, marked by a tick-mark at the left side of each frame in Fig. 2. Also presented are curves fitted to the averaged intensity values using a least-squares routine. The similarity, within 2%, in the peak values of the fluorescence induced by the KrF laser at the two sides of the test section is a quantitative demonstration that the attenuation by either absorption or trapping is negligible for the illumination, detection, and flow conditions of this experiment. This result is in agreement with a theoretical calculation⁹ where an attenuation of less than 1% for both beam and fluorescence signal was predicted for conditions typical of the present facility, i.e., OH density of $2 \times 10^{15} \text{ cm}^{-3}$ and characteristic path lengths for absorption and trapping of 10 cm. The attenuation by absorption and trapping, when the dye laser is

used, is estimated to be 70% if peak fluorescence intensities at each side of the image are compared. In the facility used in the studies, the theoretically predicted laser attenuation is 30% and the fluorescence loss is 43%. Combined, this gives a total predicted signal loss of approximately 60%.⁹ In geometrically simple cases this distortion may possibly be corrected by an iterative scheme involving the spatial variation in the LIF signal, provided the image distortion had been caused by either beam attenuation or fluorescence trapping alone. However, when both loss mechanisms are present simultaneously, the deconvolution of the individual contributions and subsequent correction for both may not be possible without a detailed knowledge of the flame properties along both the incident beam and detection paths. Furthermore, image distortion is expected to increase with OH temperature and density, becoming a severe source of error even when the imaging axis is perpendicular to the plane of the incident light-sheet.

The results of Figs. 2 and 3 demonstrate that when the concentration of OH is high, or in facilities where propagation distances are large, the application of a KrF laser may be required for quantitative or even qualitative PLIF imaging. However, the dramatic reduction in absorption and trapping associated with the use of this laser comes at the expense of reduced signal. This is evident from the lower SNR in the measurements obtained using the KrF laser system. Assuming that both measurements were limited by photon-statistical noise, the signal induced by the 84 times more powerful KrF laser was estimated to be approximately 11 times lower than the signal induced by the doubled-dye laser. With identical pulse energy, spatial resolution, and optical collection configuration, the dye laser would yield a signal 924 times greater than the KrF laser. This compares well with the theoretically predicted ratio of 1076.⁹

Conclusions

The objectives of the present work were 1) to obtain OH fluorescence planar images induced by a tunable KrF laser in supersonic H_2 -air flames, 2) to compare these images with images induced for the same conditions by a doubled-dye laser, 3) to determine the effects of absorption and radiation trapping on the results of these two LIF techniques, 4) to determine the relative signal levels of the two techniques, and 5) to compare the results with previous theoretical analysis.

Planar fluorescence images of OH in a supersonic H_2 -air flame, induced by a tunable KrF laser, were recorded. These images were compared with previously recorded²⁴ fluorescence images induced by a doubled-dye laser at identical conditions. Results indicate that the fluorescence images obtained through conventional $1 \leftarrow 0$ excitation were severely distorted by absorption and fluorescence trapping. Based on the comparison of SNR, the signal induced by the doubled-dye laser is expectedly larger than the signal induced by the KrF laser in identical flow conditions. The present measurements of the fluorescence induced by the KrF laser were controlled by the photon-statistical noise.

These results demonstrate that the application of the dye laser system for quantitative measurements in large supersonic combustion facilities is expected to be limited by attenuation of the incident beam and the strong absorption of the subsequent fluorescence that is typical of the strong transitions that are usually excited using this laser system. In flows where OH density exceeds 10^{15} cm^{-3} , excitation of the (3, 0) band by a tunable KrF laser should be used. This transition has a lower absorption coefficient than the transitions that are accessible to the dye laser system. Therefore, in most cases, the flow will appear optically thin while at the same time the elevated OH concentration will compensate for the reduced fluorescence yield. In addition, this fluorescence decay has the highest probability for transition to $v''(2)$ where radiation trapping is small.

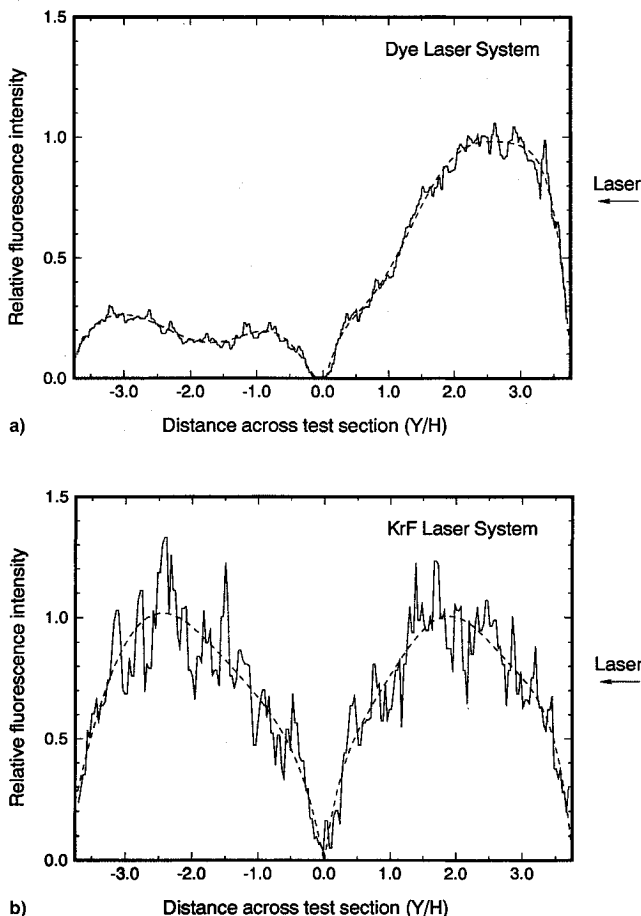


Fig. 3 Variation of the relative fluorescence intensity for the excitation-detection experiment using a) the doubled-dye laser and b) the KrF laser along a line marked on the images in Fig. 2.

Acknowledgments

This work was supported by NASA Grant NAG-1-795 from the Langley Research Center. The continued interest and support of G. Burton Northam, the technical monitor at Langley, is greatly appreciated.

References

- ¹Lee, M. P., Paul, P. H., and Hanson, R. K., "Quantitative Imaging of Temperature Fields in Air Using Planar Laser-Induced Fluorescence of O₂," *Optics Letters*, Vol. 12, No. 2, 1987, pp. 75-77.
- ²Grinstead, J. H., Laufer, G., and McDaniel, J. C., Jr., "Measurements of KrF Laser-Induced O₂ Fluorescence in High-Temperature Atmospheric Air," AIAA Paper 93-0045, Jan. 1993.
- ³Dyer, M. J., and Crosley, D. R., "Two-Dimensional Imaging of OH Laser-Induced Fluorescence in a Flame," *Optics Letters*, Vol. 7, No. 8, 1982, pp. 382-384.
- ⁴Grieser, D. R., and Barnes, R. H., "Nitric Oxide Measurements in a Flame by Laser Fluorescence," *Applied Optics*, Vol. 19, No. 5, 1980, pp. 741-743.
- ⁵Chang, A. Y., DiRosa, M. D., Davidson, D. F., and Hanson, R. K., "Rapid Tuning CW Laser Technique for Measurements of Gas Velocity, Temperature, Pressure, Density, and Mass Flux Using NO," *Applied Optics*, Vol. 30, No. 21, 1991, pp. 3011-3022.
- ⁶Chapman, G. T., "An Overview of Hypersonic Aerothermodynamics," *Communications in Applied Numerical Methods*, Vol. 4, May-June 1988, pp. 319-325.
- ⁷Rogers, R. C., "Workshop on the Application of Pulse Facilities to Hypervelocity Combustion Simulation," NASP Workshop Publication 1008, Monterey, CA, 1990.
- ⁸Andresen, P., Bath, A., Gröger, W., Lülff, H. W., Meijer, G., and Ter Meulen, J. J., "Laser-Induced Fluorescence with Tunable Excimer Lasers as a Possible Method for Instantaneous Temperature Field Measurements at High Pressures: Checks with an Atmospheric Flame," *Applied Optics*, Vol. 27, No. 2, 1988, pp. 365-378.
- ⁹Quagliaroli, T. M., Laufer, G., Krauss, R. H., and McDaniel, J. C., Jr., "Laser Selection Criteria for OH Fluorescence Measurements in Supersonic Combustion Test Facilities," *AIAA Journal*, Vol. 31, No. 3, 1993, pp. 520-528.
- ¹⁰Cattolica, R., "OH Rotational Temperature from Two-Line Laser-Excited Fluorescence," *Applied Optics*, Vol. 20, No. 7, 1981, pp. 1156-1166.
- ¹¹Crosley, D. R., "Semi-quantitative Laser-Induced Fluorescence in Flames," *Combustion and Flame*, Vol. 78, No. 1, 1989, pp. 153-167.
- ¹²Rensberger, K. J., Jefferies, J. B., Copeland, R. A., Kohse-Höinghaus, K., Wise, M. L., and Crosely, D. R., "Laser-Induced Fluorescence Determination of Temperatures in Low Pressure Flames," *Applied Optics*, Vol. 28, No. 17, 1989, pp. 3556-3566.
- ¹³Barlow, R. S., and Collignon, A., "Linear LIF Measurements of [OH] in Nonpremixed Methane-Air Flames: When Are Quenching Corrections Unnecessary," AIAA Paper 91-0179, Jan. 1991.
- ¹⁴Cattolica, R. J., and Vosen, S. R., "Two-Dimensional Measurements of the [OH] in a Constant Volume Combustion Chamber," *20th Symposium on Combustion*, Combustion Inst., Pittsburgh, PA, 1984, pp. 1273-1282.
- ¹⁵Allen, M. G., Parker, T. E., Reinecke, W. G., Legner, H. H., Foutter, R. R., Rawlins, W. T., and Davis, S. J., "Instantaneous Temperature and Concentration Imaging in Supersonic Air Flow Behind a Rear-Facing Step with Hydrogen Injection," AIAA Paper 92-0137, Jan. 1992.
- ¹⁶Seitzman, J. M., Palmer, J. L., Antonio, A. L., and Hanson, R. K., "Instantaneous Planar Thermometry of Shock-Heated Flows Using PLIF of OH," AIAA Paper 93-0802, Jan. 1993.
- ¹⁷Seitzman, J. M., and Hanson, R. K., "Comparison of Excitation Techniques for Quantitative Fluorescence Imaging of Reacting Flows," *AIAA Journal*, Vol. 31, No. 3, 1993, pp. 513-519.
- ¹⁸Drier, T., Dreizler, A., and Wolfrum, J., "The Application of a Raman-Shifted Tunable KrF Excimer Laser for Laser-Induced Fluorescence Combustion Diagnostics," *Applied Physics B*, Vol. 55, No. 4, 1992, pp. 381-387.
- ¹⁹Lengel, R. K., and Crosely, D. R., "Energy Transfer in A²Σ⁺ OH. II. Vibrational," *Journal of Chemical Physics*, Vol. 68, No. 12, 1978, pp. 5309-5324.
- ²⁰Barlow, R. S., Dibble, R. W., and Lucht, R. P., "Simultaneous Measurement of Raman Scattering and Laser-Induced OH Fluorescence in Nonpremixed Turbulent Jet Flames," *Optics Letters*, Vol. 14, No. 5, 1988, pp. 263-265.
- ²¹Sink, M. L., and Bandrauk, A. D., "Theoretical Analysis of the Predissociation of the A²Σ⁺ State of OH," *Journal of Chemical Physics*, Vol. 73, No. 9, 1980, pp. 4451-4459.
- ²²Hiller, B., Paul, P. H., and Hanson, R. K., "Image-Intensified Photodiode Array as a Fluorescence Detector in CW-Laser Experiments," *Review of Scientific Instruments*, Vol. 61, No. 7, 1990, pp. 1808-1815.
- ²³Laufer, G., McKenzie, R. L., and Fletcher, D. G., "Method for Measuring Temperatures and Densities in Hypersonic Wind Tunnel Air Flows Using Laser-Induced O₂ Fluorescence," *Applied Optics*, Vol. 29, No. 33, 1990, pp. 4873-4883.
- ²⁴Abitt, J. D., III, Segal, C., McDaniel, J. C., Jr., Krauss, R. H., and Whitehurst, R. B., "Experimental Supersonic Hydrogen Combustion Employing Staged Injection Behind a Rearward-Facing Step," *Journal of Propulsion and Power*, Vol. 9, No. 3, 1993, pp. 472-478.